Journal of Applied Fluid Mechanics, Vol. 17, No. 5, pp. 980-988, 2024.
Available online at www.jafmonline.net, ISSN 1735-3572, EISSN 1735-3645.
https://doi.org/10.47176/jafm.17.05.2347

Acoustic Noise Measurement Downstream of an Oscillating Wind Turbine Blade Section

A. R. Davari † and S. Hadavand

Department of Engineering, Tehran Science and Research Branch, Islamic Azad University, Poonak, Tehran, 14155-4933, Iran

†*Corresponding Author Email: ardavari@srbiau.ac.ir*

ABSTRACT

Acoustic measurements were performed using microphone downstream of a 2-D wind turbine blade section in wind tunnel. The experiments have been carried out in both static and oscillatory pitching cases. The latter is usually experienced by the blades in actual circumstances. The microphone was 1.5 chords downstream of the airfoil and the measurements were conducted at three transverse positions, i.e. behind the trailing edge, midway between the trailing edge and the ground and very close to the ground. A CFD simulation of the flowfield has also been conducted using Fluent to correlate the acoustic behavior to the phenomena observed in the flowfield around the blade. The results show that the acoustic noise heard by a listener located on the ground is higher and stronger than that positioned downstream of the trailing edge, showing the ground effect on acoustic noise reverberation. The aerodynamic noise heard by the listener, changes from a treble to bass sound as the angle of attack increases. Beyond stall, the flow is dominated by the vortices shed into wake and the acoustic noises would be at very low frequencies which would result in a bass sound accompanied by structural vibration. In high angle of attack range, such noises can hardly be heard by a normal person but have a very destructive role on blade structure.

Article History

Received September 29, 2023
Revised November 27, 2023
Accepted December 11, 2023
Available online February 24, 2024

Keywords:

Sound Amplitude
Sound Pressure Level
Aeroelastic
Power Spectrum
Trailing edge

1. INTRODUCTION

A large number of complex flow phenomena occur in a wind turbine blade, each generating sound in particular frequency bands. Among the various sources of sound in a wind turbine, the aerodynamic noise associated with the passage of air over the blades is typically the most important component of acoustic emissions, Tonin (2012). This noise is caused by the interaction of the turbulent boundary layer eddies with the trailing edge of the wind turbine blade, Merino-Martínez et al. (2021).

According to various noise guidelines and standards, there is a level of "swish" which is a normal characteristic of wind turbines. However, an increased level of amplitude modulation is reported as Impulsive Noise. There is still little knowledge about the mechanism of the impulsive noise and the conditions that are responsible for it, Li et al. (2020).

Bhargava and Samala (2019) has simulated the acoustic emissions from wind turbine blades for a three-bladed horizontal axis 3 MW turbine using a quasi-empirical model. He observed that most of trailing edge noise source is produced from the outboard sections and during downward motion of the blade.

Bertagnolio et al. (2016) proposed a model to predict wind turbine noise, based on a standard wind turbine aeroelastic code for various noise models. They pointed out that the trailing edge is the major contributor to the overall acoustic noise at low wind speeds and high frequencies.

In the recent years, with the advent of modern computer software and hardware including processors and computational algorithms, numerical simulations for wind turbine noise sources have been brought to the forefront of the aero-acoustic calculations. Several numerical simulations using LES and the Ffowcs-Williams and Hawkings, FW–H, acoustic analogy, Wasala et al. (2015), Su et al. (2019) and Dai and Li (2019) in the wake region of wind turbine blades have revealed that as increasing the tip speed ratio and consequently the loads on blades, larger thickness and loading noise are generated which are the dominant noise sources. It has also been pointed out that the peaks of acoustic pressure levels move toward the center of the blade as increasing the tip speed, while in the tip eddy region, they migrate outwards.

NOMENCLATURE

α	angle of attack in static tests.	Re	Reynolds number based on chord length
α_o	mean angle of attack in dynamic tests.	$k=\pi fc/V_\infty$	reduced frequency
α_A	oscillation amplitude in dynamic tests	I	sound intensity
c	chord length	p	local instantaneous sound pressure measured by the microphone

Several investigations have also been devoted to the acoustic noise measurement and reduction in wind turbines. Arnold et al. (2018) have put forward a method to design a boundary-layer suction system for turbulent trailing-edge noise reduction. Within a certain design regime, a trailing-edge noise reduction was pointed out, accompanied by an enhancement of the rotor power. However, under the conditions at which the suction power requirement compensates the amelioration of the aerodynamic power, a trade-off between aeroacoustics and the aerodynamic performance arises.

In recent surveys, Maizi et al. (2018), Deshmukh et al. (2019), Volkmer et al. (2021) and Cao et al. (2021), some passive flow control policies on wind turbine blades have been examined to decrease the aerodynamic noise namely, optimization of the blade profile, boundary layer tripping and the serrated trailing edge. It has been concluded that the aerodynamically optimized blades with trailing edge serrations, even without any boundary layer trip, provide the best compromise between noise reduction and degradation of the aerodynamic performance.

All sources of noise in a wind turbine are subjected to the ground effect. It can change wind turbine sound levels by several decibels and can vary considerably among turbine locations, depending upon the ground composition in the vicinity of the noise receivers, Dijkstra (2015).

Up to now, valuable information has been obtained about role of the ground effect in acoustic noise propagation. However in various working conditions of a wind turbine blade, particularly when the blade experiences such structural oscillations as flapping, pitching or a combination of them, there is still a long way to discover and explain the wind turbine noise production and propagation processes.

The Sound pressure level, SPL, is the pressure level of a sound, measured in decibels, dB. It can be calculated from the sound pressure as:

$$\mathrm{SPL} = 20\log\frac{p^2}{p_{ref}^2} \qquad (1)$$

Where p is the root mean square, rms, of sound pressure and p_{ref} is the threshold of human hearing at about 1000 Hz. Obviously, when the sound pressure is equal to the reference pressure the SPL would be zero dB. The SPL is normally expressed in frequency domain, Wagner et al. (1996).

Sound waves can have the same SPL but a different frequency. In such cases, these tones are also perceived as being of different volumes. Therefore, the parameter sound intensity is also defined to be measurable as a purely subjective quantity. The sound waves contain energy as do the electro-magnetic waves. The sound intensity is the amount of energy per unit time displaced from a unit area or equivalently, the energy power per unit area. It is defined as the square of the rms pressure divided by the acoustic impedance, Wagner et al. (1996). The latter is the product of density and the speed of sound in the fluid under consideration.

In this paper, an experimental survey has been undertaken to measure the acoustic noise downstream of a 2D wind turbine blade section oscillating in pitch. Both the sound intensity and the sound pressure level have been calculated from the acoustic pressure values recorded by the microphone. The measurements were for various elevations from the blade trailing edge. A numerical simulation has also been performed on the same airfoil to describe the flow pattern at various conditions and correlate the measured noises to the aerodynamic flowfield over the airfoil.

2. EXPERIMENTAL SETUP AND PROCEDURE

The experiments were performed in a subsonic closed return type wind tunnel with test section dimensions of 80×80 cm² and the maximum attainable speed in the test section is 100 m/sec. According to hot wire measurements, the turbulence intensity in the test section is less than 0.1%.

The model was NACA 63415 airfoil which has been widely used in wind turbine blade sections, for instance in Bounus Combi 300 kW wind turbine, Fuglsang and Madsen (1998). In the mechanism used for oscillating the model, the rotational motion of an electric motor was converted through a crank shaft, joints and connecting rods into the reciprocating motion. The pivot point in the present experiments was at the quarter chord of the model and the oscillation frequency was controlled by the motor rotational speed. The oscillation amplitude could be set by adjusting the joints and the connecting rods, Davari (2017).

Figure 1 shows the model installed in the test section and the mechanism manufactured to oscillate the model in pitch. The model span was 80 cm and its chord length was 25 cm. The experiments have been performed at a single Reynolds number of 1.6×10^6. The static tests were at the angles of attack of 5, 12, 18 and 20 degrees. The dynamic pitching tests have been undertaken at a constant reduced frequency of 0.092 and the oscillation amplitude of ±2°. The mean angles of attack in dynamic tests were 12, 18 and 20 degrees.

The maximum blockage ratio in the present experiments has been calculated to be about 5.5% at the maximum instantaneous angle of attack during the oscillatory pitching motion. In the present experiments, 5

Fig. 1 The 2D turbine blade installed in the test section along with the oscillation mechanism

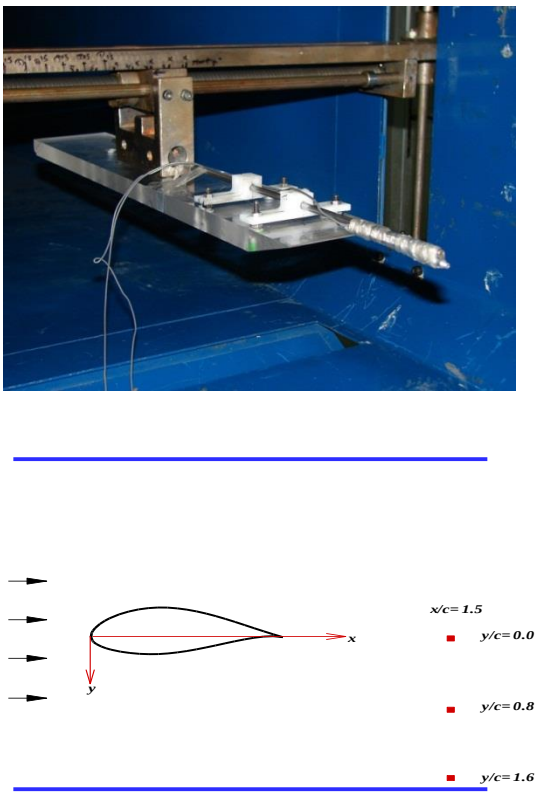

Fig. 2 Microphone setup and the measurement points downstream of the model

and 3 repetition tests have been performed for some of the static and dynamic cases, respectively. Within 95% confidence level and calculating the mean and standard deviations and also using the t-student value, the maximum uncertainty in static and dynamic measurements have been calculated to be ±7.5% and ±10%, respectively.

A PCB378B02 microphone with a frequency range from 3.75 Hz up to 20 kHz and sensitivity of 50 mV/Pa with 1/2" ICP® preamplifier 426E01 and TEDS equipped with a nose cone adaptor has been employed to measure the acoustic noise downstream of the airfoil inside the test section.

The measurements have been performed both with the model inside the test section and in the absence of the model to record the background noises including the wind tunnel and the oscillation mechanisms as well as the ambient and the microphone inherent noise signals. The microphone installed on the traversing downstream of the model and the schematic view of the measurement points are shown in Fig. 2.

In the present experiments, the microphone was 1.5 chords away from the airfoil and the measurements were conducted at three transverse positions, i.e y/c=0.0 behind the trailing edge, y/c=0.8 midway between the trailing edge and the ground and finally at y/c=1.6 very close to the ground.

The data acquisition system was brought as close as possible to the microphone to shorten the amount of analogue microphone cabling required. This has also provided significant cost savings on expensive high-quality transducer cables, fewer setup and measurement errors due to reduced cable infrastructure, and a higher signal quality. The data were acquired by AT-MIO-64E-3 data acquisition board capable of scanning 64 channels at a maximum rate of 500 kHz. For the present experiments, 300 and 900 samples per second have been acquired for static and dynamic tests respectively.

Though no data was found in the literature on the aero-acoustic behavior of this airfoil, some aerodynamic parameters were compared to check the validity of the numerical simulations in this paper as well as the present wind tunnel data.

In addition to the acoustic measurements, the surface pressure on the airfoil has been individually measured in the wind tunnel using 29 differential pressure transducers. Because of the high-pressure gradients near the leading edge, the sensors at the front half were of ±5 psi range and for the rear half, ±1 psi sensors were exploited. The response time of the sensors were 1 milli sec. Shown in Fig. 3(a) are the schematic view of the pressure taps location on the airfoil and one of the transduces used for pressure measurements.

Figure 3(b) shows the surface pressure measurement at a static angle of attack of 5 degrees. The present numerical simulations result on this airfoil has been compared to that of Bak et al. (2000). Comparing the numerical and experimental pressure values obtained in this paper with those found in Ref. 18 shows a good agreement and approves that the experimental setup along with the numerical simulations for this airfoil in the present paper is satisfactorily accurate. In dynamic case, only the present experimental and numerical data were compared.

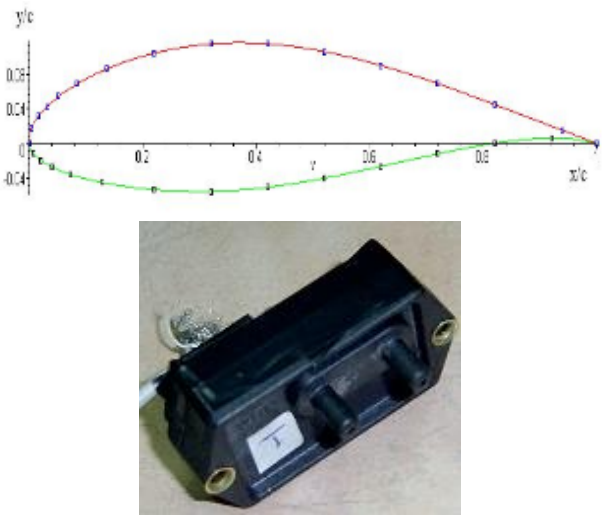

(a) The pressure taps location on the model and the pressure transducer used for surface measurement

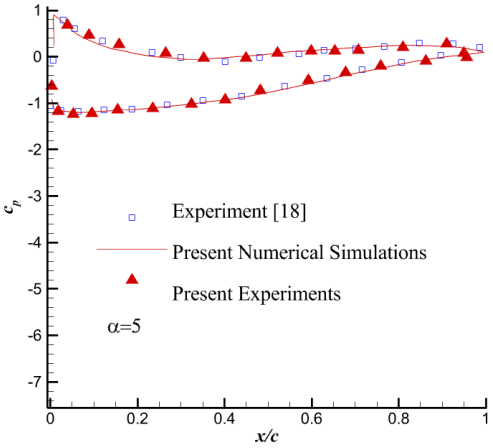

(b) pressure distribution in static case, α=5°

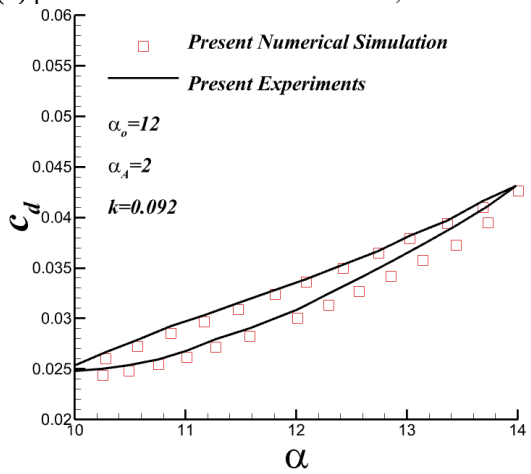

(c) variations of drag coefficient with instantaneous angle of attack in dynamic tests

Fig. 3 Data validity check

The surface pressure measured during pitching motion in the present experiments has been integrated to calculate the pressure drag at various dynamic angles of attack. Comparing these values with the drag coefficients obtained from the numerical simulations shows a good agreement, Fig. 3(c). However, note that the numerical data are the total drag whereas the experimental results are the pressure drag only. For this reason, the numerical drag

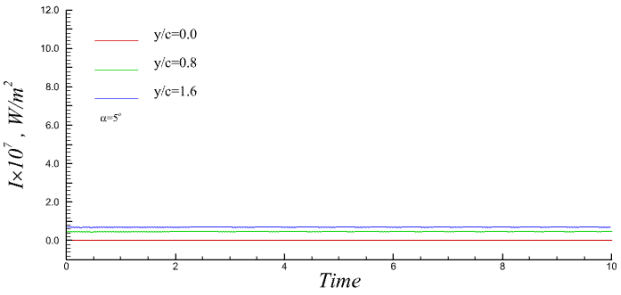

(a) The sound intensity

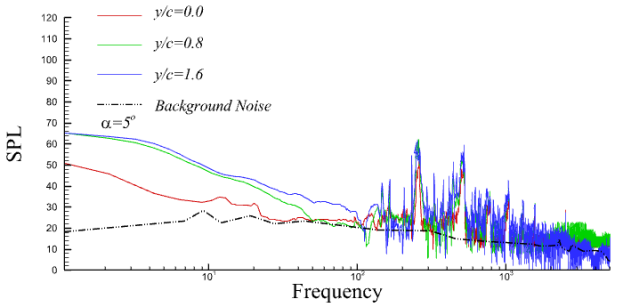

(b) The sound pressure level

Fig. 4 Acoustic measurements downstream the airfoil at α=5°

is slightly more than the experimental one. For this range of the angle of attack, the pressure term is the major contributor to the overall drag.

3. RESULTS AND DISCUSSIONS

The experiments were performed for both static and dynamic pitching motions for various mean angles of attack and at a constant pitching frequency and amplitude of ±2° to simulate the aeroelastic torsional motion of the blade in actual circumstances.

3.1 Static Results

Shown in Fig. 4 are the acoustic measurement results downstream of the airfoil at α=5°. For this angle of attack, the sound intensity is very weak in the form of a weak noise or whisper. At the training edge this noise is vanishingly small. However, as traveling down toward the ground, the intensity is amplified and some signatures of fluctuations can be observed. The sound pressure level in Fig. 4(b) shows that these fluctuations have frequency modes above about 100 Hz, below which, a monotonic behavior is evident. A frequency mode at about 15 Hz can be detected in front of the trailing edge. This single acoustic mode is likely due to the small disturbances in flow leaving the sharp trailing edge.

A numerical simulation, using Ansys Fluent, has also been performed to investigate the flowfield over the airfoil and correlate it to the acoustic field. The computational domain in numerical simulation has been considered wide enough to not imply unwanted flow reflection. Unstructured grids were generated around the airfoil in this paper. However, within the boundary layer, the structurally inflated meshes were employed to adequately simulate the effect of turbulent viscosity. Figure 5(a)

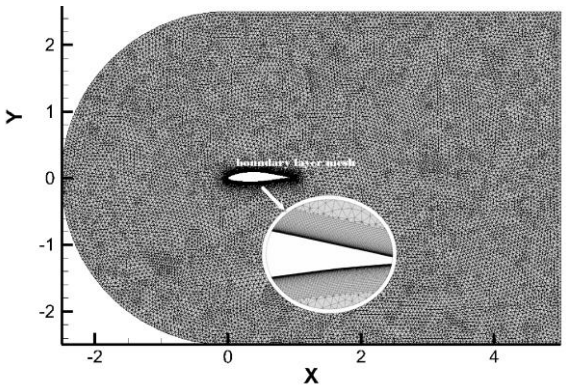

(a) The computational domain at α=0,

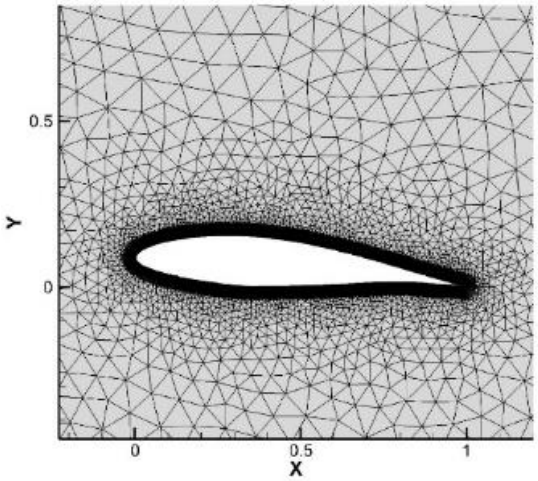

(b) The computational domain at α=5,

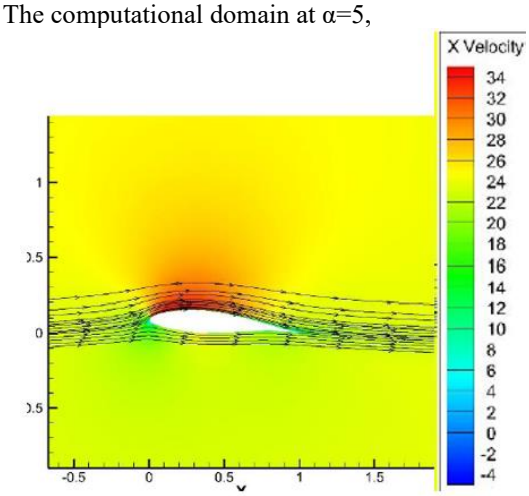

(c) the stream lines at α=5º

Fig. 5 Numerical simulation result at α=5º

shows the computational domain for the airfoil at zero angle of attack. For non-zero angles of attack, for instance at α=5, 444121 high density triangular meshes were employed and the distance between the first mesh layer and the surface corresponded to y^+<0.8. This has been shown in Fig. 5(b). The kω-SST turbulence model was used for this simulation. From Fig. 5(c) no separation or irregular patterns can be observed in the flowfield. This causes a smooth acoustic behavior downstream.

Figure 6 shows the flow pattern over the airfoil at α=12º. An attached separation bubble can be detected in the vicinity of the trailing edge which decreases the lift. However, it does not seem to have any influence on acoustic behavior.

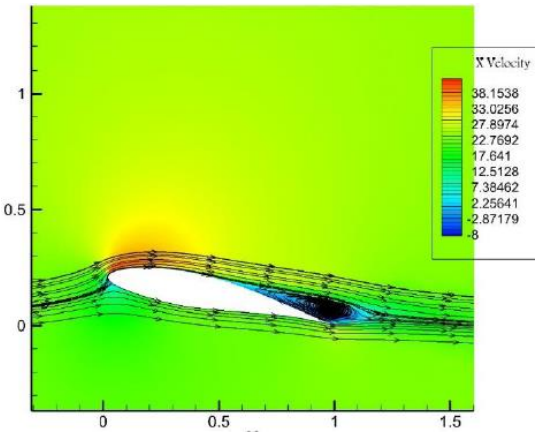

Fig. 6 Numerical simulation result at α=12º

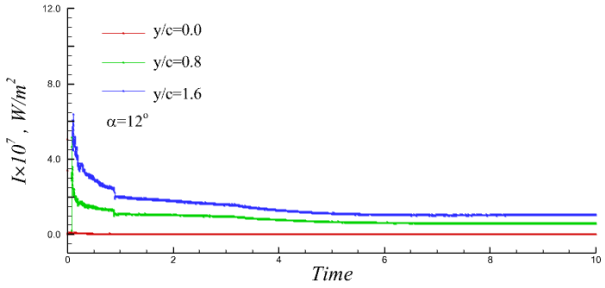

(a) The sound intensity

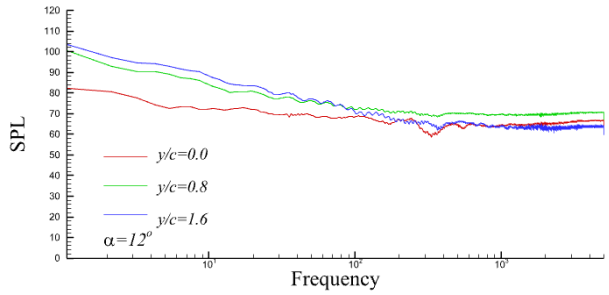

(b) The sound pressure level

Fig. 7 Acoustic measurements downstream the airfoil at α=12º

Shown in Fig. 7 are the acoustic parameters at α=12º. The sound intensity at y/c=0.8 and 1.6 has been remarkably increased while near the trailing edge still remained negligible. This shows ground effect on noise propagation which amplifies the acoustic noise below the airfoil where the high pressure flow at the lower surface is dominant. Here the frequency modes start at about 20 Hz and very low sound pressure levels are observed at very high frequencies.

For the angle of attack of 18º, the flow separation and the highly turbulent boundary layer do affect the acoustic behavior. In this case, the mesh number has been increased to 929740 rectangular grids with an aspect ratio near to 1.0. Figure 8 shows the flowfield at α=18º in which the separation bubble has been burst and the vortex shedding into the wake region is evident.

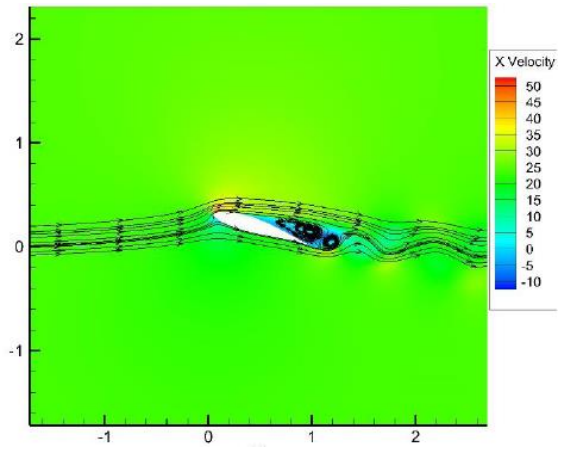

Fig. 8 Numerical simulation result at α=18º

According to Fig. 9, the sound intensity has been increased and the periodic behavior is directly affected by the separated flow vortex shedding from the trailing edge. When moving downward at y/c=0.9, the oscillation amplitude decreased and near the ground the sound intensity and its oscillation amplitude increased remarkably. This is the acoustic noise reverberation near the ground and shows the mechanism of noise propagation by the ground effect. The variations of SPL, Fig. 9(b), suggests that at α=18º, the frequency modes occur at lower frequencies in the form of bass sound. The first peak in frequency spectrum occurred at 20 Hz which is the threshold for human hearing. Thus the acoustic noise at the angles of attack below about 18º cannot be clearly heard by the human ear and at α=18º a listener can hear a weak treble sound, especially when located downstream of the blade on the ground. This is due to interaction of the turbulent and separated boundary layer with the trailing edge which creates a sound like Woosh in the flow accompanied by some high frequency treble weaker sounds.

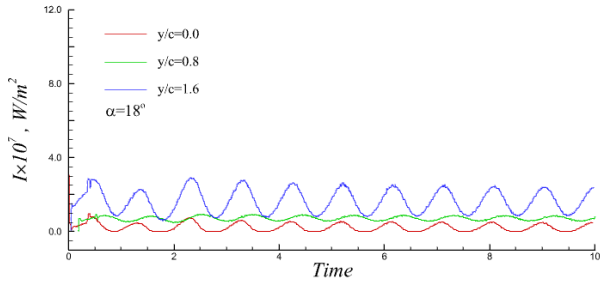

(a) The sound intensity

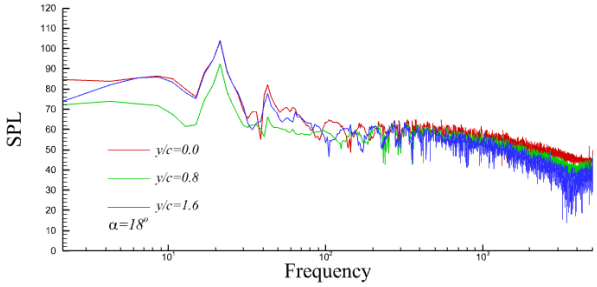

(b) The sound pressure level

Fig. 9 Acoustic measurements downstream the airfoil at α=18º

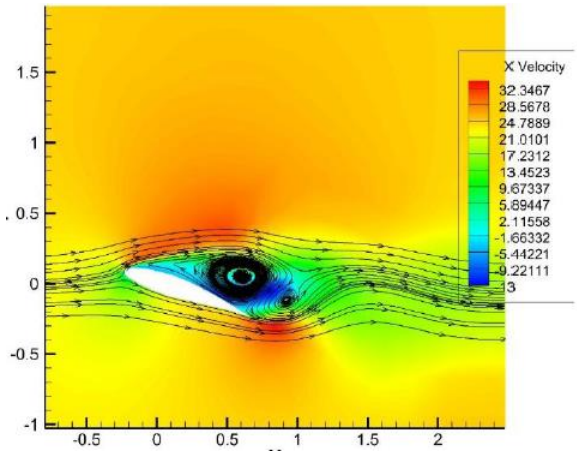

Fig. 10 Numerical simulation result at α=20º

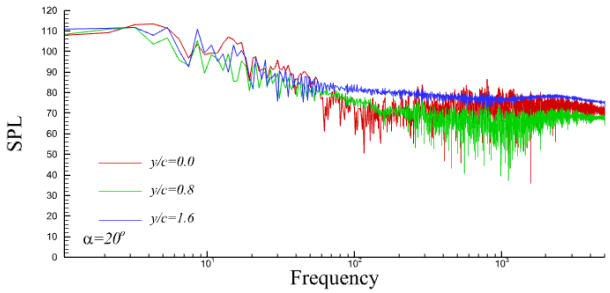

Fig. 11 Sound pressure level downstream the airfoil at α=20º

For α=20º the vortex shedding into the wake increases and gives rise to the acoustic noise. A less dense mesh has been employed here with y+ less than about 0.7. The flowfield in this case, shown in Fig. 10, is dominated by a strong separation bubble and has a remarkable impact on the downstream acoustic field.

Shown in Fig. 11 is the sound pressure level at α=20º. The noise level has been evidently increased comparing to the corresponding values at α=18º due to post stall vortex shedding. In this case the bass sound is completely in the range of hearing and a listener hears a clear bass sound along with stronger treble high frequency sounds. Note that in this case a listener standing downstream on the ground receives lower amplitude higher pressure levels than the one located just behind the airfoil trailing edge or even midway between the airfoil and the ground. The SPL values in this case are as high as the noise heard in a subway from platform.

3.2 Dynamic Results

As stated earlier, in dynamic tests the airfoil was in a sinusoidal pitching motion at a reduced frequency of 0.092 and the oscillation amplitude of ±2º. The oscillations were about the mean angles of attack of 12, 18 and 20 degrees. This pitching motion could be a simulation of the torsional blade oscillations for a real wind turbine during operation.

In dynamic CFD simulations, the meshes were more condensed than those in static case. A circular zone around the airfoil, whose center was at the quarter chord, was

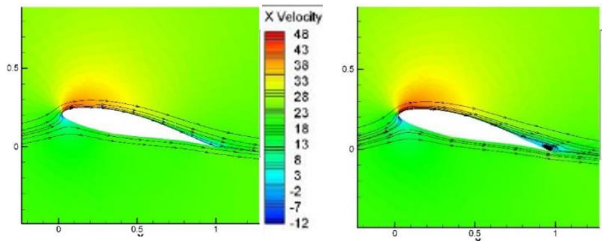

(a) Upstroke, α=12.02º (b) Upstroke, α=13.37º

(c) Downstroke, α=13º (d) Downstroke, α=13.48º

Fig. 12 Streamline over the airfoil at typical time steps, αo=12º

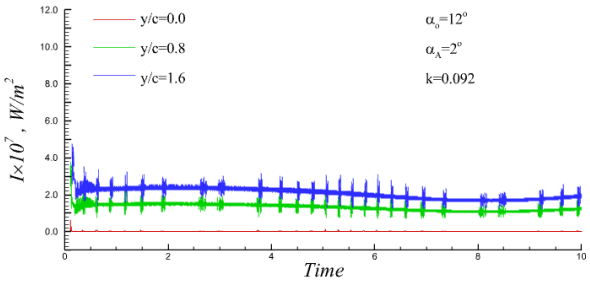

(a) The sound intensity

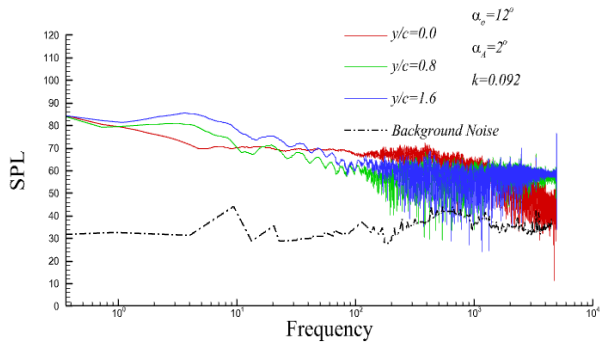

(b) The sound pressure level

Fig. 13 Acoustic measurements downstream the pitching airfoil at αo=12º

provided to oscillate in pitch. The average mesh aspect ratio was 0.87.

In pitching motion about 12º mean angle of attack, the attached separation bubble has been appeared at about 13º upstroke motion which has not been bust throughout the oscillation cycle. For the angle of attack of 18º, the flow separation and the highly turbulent boundary layer do affect time steps have been shown in Fig. 12.

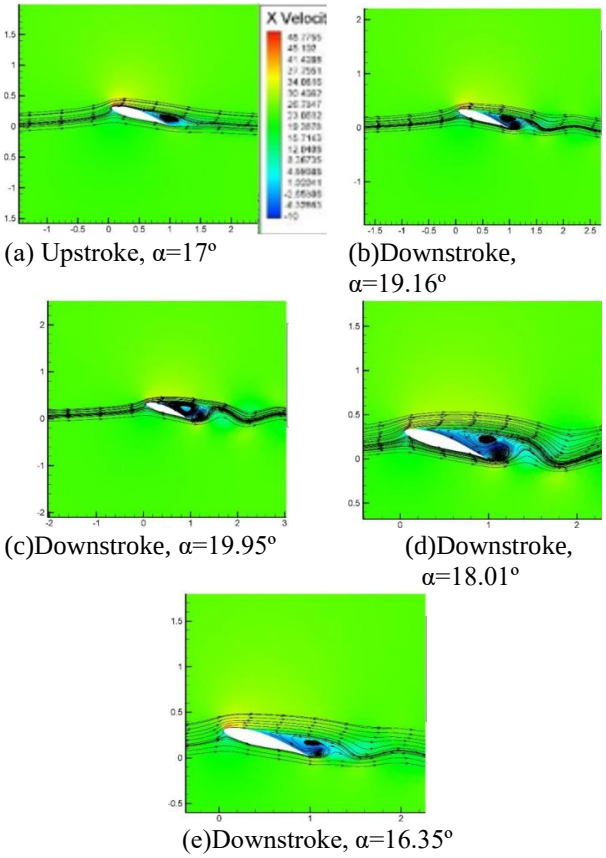

(a) Upstroke, α=17º (b)Downstroke, α=19.16º

(c)Downstroke, α=19.95º (d)Downstroke, α=18.01º

(e)Downstroke, α=16.35º

Fig. 14 Streamline over the airfoil at typical time steps, αo=18º

The sound intensity shown in Fig. 13(a) has patterned harmonic fluctuations in contrast to the corresponding static case which is evidently the signature of the unsteady flow at the trailing edge and the interaction of the attached bubble with the sharp trailing edge. The intensity increases near the ground. Note that the amplitude of the fluctuation increases as moving down towards the ground.

The high-frequency modes in SPL in Fig. 13(b) also are an indication of the unsteady periodic motion of the model. The strong modes are at the frequencies higher than 100 Hz. Comparing with the static case, it can be inferred that a listener on the ground below and downstream of the oscillating blade hears a bass sound which is not too annoying, while hears nearly nothing when the blade is in static condition.

At the mean angle of attack of 18º in static case a frequency jump has been observed at 1000 Hz. For the dynamic pitching case, a triangular mesh using 401239 cells have been generated around the airfoil. According to Fig. 14, the instantaneous angle of attack range between 17.3º to 18º seems to be the dynamic stall onset. The SPL and the sound intensity in Fig. 15 show a remarkable increase in noise comparing to αo=12º which approves that αo=18º is a critical angle from both aerodynamics and acoustics points of view.

Similar to αo=12º, the sound intensity increases near the ground. The sound pressure level in Fig. 15(b) shows that the high amplitude modes occur at low frequencies and thus a bass sound is heard by the listener when the airfoil oscillates in stall range. The average sound pressure

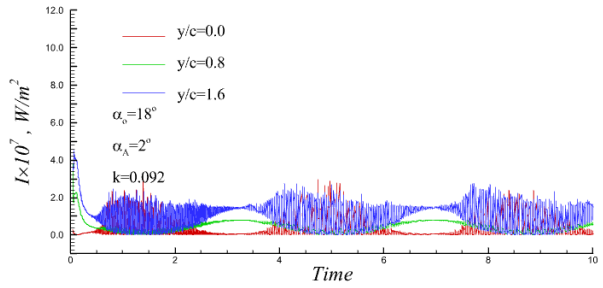

(a) The sound intensity

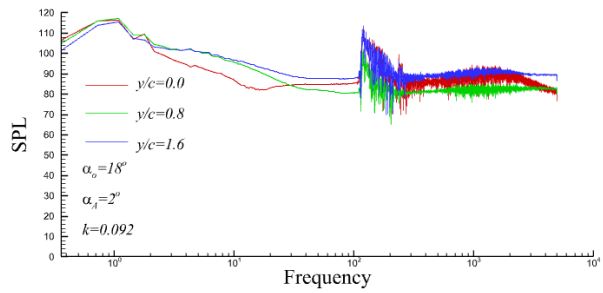

(b) The sound pressure level

Fig. 15 Acoustic measurements downstream the pitching airfoil at αo=18º

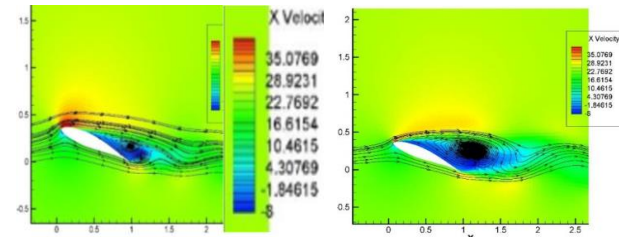

(a) Upstroke, α=19.03º (b) Upstroke, α=21.09º

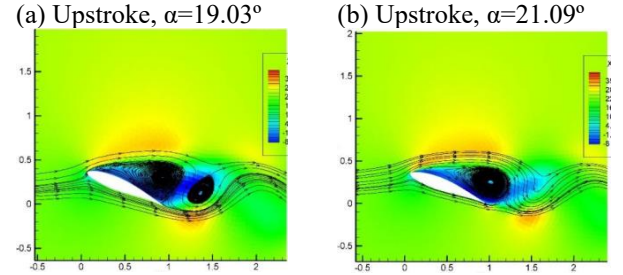

(c) Downstroke, α=21.47º (d) Downstroke, α=19.36º

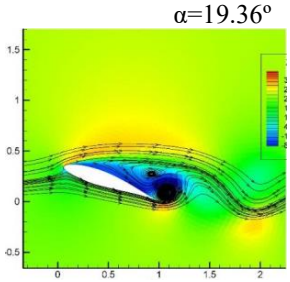

(e) Downstroke, α=18.0º

Fig. 16 Streamline over the airfoil at typical time steps, αo=20º

level in this case was about 100 dB which is equivalent to the noise generated by a circular saw located 3 ft apart.

Note that in the corresponding static test, the average SPL was about 70 dB and the oscillations have been occurred

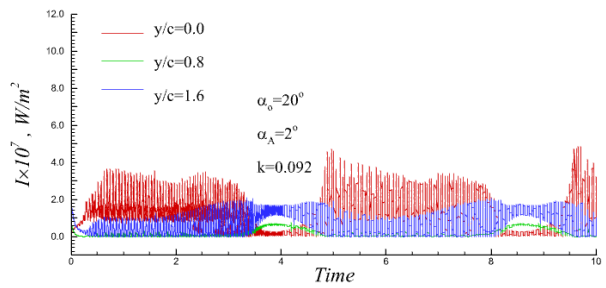

(a) The sound intensity

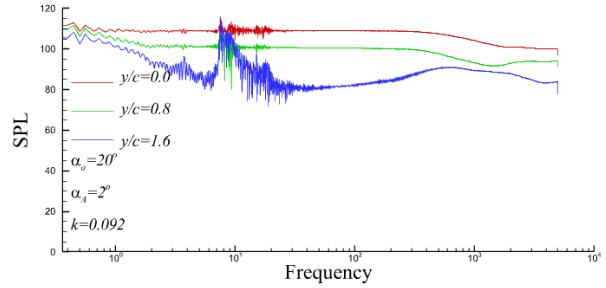

(b) The sound pressure level

Fig. 17 Acoustic measurements downstream the pitching airfoil at αo=20º

at high frequencies while in oscillatory motion, the fluctuations have been attenuated and damped at higher frequencies. This might be attributed to dynamic stall and flow separation in this angle of attack range.

For post stall region at α_o=20º, Fig. 16 shows that during both upstroke and downstroke motions, the flow is entirely detached from the upper surface. The fluctuations in SPL, shown in Fig. 17, occurred at very low frequencies and thus a strong bass sound would be heard. Note that unlike the previous cases examined earlier, the overall sound pressure level for beyond stall range has not been amplified by the ground effect. However, the ground still played its role in sound fluctuations.

4. CONCLUSION

A series of acoustic measurements was performed by a microphone downstream of a wind turbine blade section oscillating in pitch in the wind tunnel. Some numerical investigations were also conducted on the same blade section to study the instantaneous flow field and correlate it to the experimental acoustic measurements. The results show that as increasing the angle of attack, the oscillatory modes in SPL power spectrum shift from high frequencies to low ones and the sound level received near the ground is higher than that in the vicinity of the trailing edge. From the frequency band it can be deduced that the aerodynamic noise, heard by the listener, changes from a treble to bass sound as the angle of attack increases. This has been observed in both static and dynamic tests. In post stall range where the upper surface experiences a severe separation, the oscillatory modes have been observed at very low frequencies which would result in a bass sound along with structural vibration. In this angle of attack range or higher, a monotonic bass noise is dominated which may not be easily and clearly heard but can have a

very destructive role on blade structure during long time operation. The oscillatory pitching motion do affect the acoustic behavior especially in near and post stall regions where the flow is strongly dominated by the vortices shed downstream into wake region. During pitching motion at low angles of attack, some constant oscillatory modes were detected in the band of 1.5 to 2.5 kHz which can be deemed to be the inherent noises due to presence of the blade section itself and also the interaction of the turbulent boundary layer and the sharp trailing edge which makes a sound like Woosh.

CONFLICT OF INTEREST

The authors state that they have no conflicts to disclose.

AUTHORS CONTRIBUTION

A. R. Davari: Conceptualization, Writing – review & editing; **S. Hadavand**: Investigation, Writing – original draft.

REFERENCES

Arnold, B., Lutz, T. H., & Krämer, E. (2018). Design of a boundary-layer suction system for turbulent trailing-edge noise reduction of wind turbines. *Renewable Energy*, *123*, 249-262. https://doi.org/10.1016/j.renene.2018.02.050

Bak, C., Fuglsang, P., Johansen, J., & Antoniou, I. (2000). *Wind tunnel tests of the NACA 63-415 and a modified NACA 63-415 Airfoil*, Risø National Laboratory, 1193(EN), Denmark, ISBN 87-550-2716-4. https://doi.org/10.2514/6.2017-4626

Bertagnolio, F., Madsen, H. A., Fischer, A., & Bak, C. (2016, April 10-15). *Validation of an aero-acoustic wind turbine noise model using advanced noise source measurements of a 500 kW turbine*. International Symposium on Transport Phenomena and Dynamics of Rotating Machinery, Hawaii, Honolulu. https://hal.science/hal-01891317

Bhargava, V., & Samala, R. (2019). Acoustic emissions from wind turbine blades. *Journal of Aerospace Technology Management*, *11*, 1458-1467. https://doi.org/10.5028/jatm.v11.1071

Cao, H., Zhang, M., Zhang, Y., & Zhou, T. (2021). A general model for trailing edge serrations simulation on wind turbine airfoils. *Theoretical and Applied Mechanics Letters*, *11*(4), 100284. https://doi.org/10.1016/j.taml.2021.100284

Dai, Y., & Li, B. (2019). A numerical study of the acoustic radiation characteristics of the aerodynamic noise in the near-wake region of a wind turbine. *Results in Physics*, *15*, 257-269. https://doi.org/10.1016/j.rinp.2019.102782

Davari, A. R. (2017). Wake structure and similar behavior of wake profiles downstream of a plunging airfoil. *Chinese Journal of Aeronautics*, *30*(4), 1281–1293. https://doi.org/10.1016/j.cja.2017.05.007

Deshmukh, S., Bhattacharya, S., Akshoy, A., & Paul, R. (2019). Wind turbine noise and its mitigation techniques: A review. *Energy Procedia*, *160*, 633-640. https://doi.org/10.1016/j.egypro.2019.02.215

Dijkstra, P. W. (2015). *Rotor noise and aero-acoustic optimization of wind turbine airfoils*. [MSc Thesis, Delft University of Technology]. http://dx.doi.org.proxy.lib.utk.edu:90/10.1007/978-3-540-71343-2

Fuglsang, P., & Madsen, H. A. (1998). Wind turbine design with numerical optimization and a semi-empirical noise prediction model. *Wind Engineering*, *22*(1), 31–41. https://www.jstor.org/stable/43749913

Li, J., Liu, R., Yuan, P., Pei, Y., Cao, R., & Wang, G. (2020). Numerical simulation and application of noise for high-power wind turbines with double blades based on large eddy simulation model, *Renewable Energy*, *146*(1), 1682-1690. 10.1016/j.renene.2017.10.058

Maizi, M., Mohamed, M. H., Dizene, R., & Mihoubi, M. C. (2018). Noise reduction of a horizontal wind turbine using different blade shapes. *Renewable Energy*, *117*, 242-256. https://doi.org/10.1016/j.renene.2017.10.058

Merino-Martínez, R., Pieren, R. & Schäffer, B. (2021). Holistic approach to wind turbine noise: From blade trailing-edge modifications to annoyance estimation, *Renewable and Sustainable Energy Reviews*, *148*(2), 111285. https://doi.org/10.2514/1.C035655

Su, J., Lei, H., Zhou, D., Han, Z., Bao, Y., Zhu, H., & Zhou, L. (2019). Aerodynamic noise assessment for a vertical axis wind turbine using improved delayed detached eddy simulation, *Renewable Energy*. *141*, 559-569. https://doi.org/10.1016/j.renene.2019.04.038

Tonin, R. (2012). Sources of wind turbine noise and sound propagation. *Acoustics Australia*, *40*(1), 3376-387. https://doi.org/10.1007/s40857-017-0098-3

Volkmer, K, Kaufmann, N., Carolus, T. H. (2021). Mitigation of the aerodynamic noise of small axial wind turbines-methods and experimental validation. *Journal of Sound and Vibration*, *500*, 116027, 468-480. https://doi.org/10.1016/j.jsv.2021.116027

Wagner, S. J., Bareiss, R., & Guidati, G. (1996). *Wind turbine noise*, Springer. https://doi.org/10.1007/978-3-642-88710-9

Wasala, S. H., Storey, R. C., Norris, S. E. & Cater, J. E. (2015). Aeroacoustic noise prediction for wind turbines using Large Eddy Simulation. *Journal of Wind Engineering and Industrial Aerodynamics*, *145*, 17-29. https://doi.org/10.1016/j.jweia.2015.05.011